

## Liquid $^3\text{He}$ . III. The Binding Energy and Other Properties at Zero Temperature\*

E. Østgaard<sup>†</sup>

*Palmer Physical Laboratory, Princeton University, Princeton, New Jersey*  
(Received 7 June 1968; revised manuscript received 25 September 1968)

The binding energy of liquid  $^3\text{He}$  is estimated by separate calculations of the two-body and the three-body interaction energy. The two-body contribution is calculated by means of Brueckner theory, using a modified Brueckner-Gammel method. The approximation of a reference energy spectrum with an effective mass and quadratic momentum dependence is used for the input single-particle energy spectrum. The intermediate-state potential energies off the energy shell are chosen to be equal to zero, and the outer self-consistency requirement in the Brueckner method is neglected. A self-consistent solution is obtained, however, by the requirement that the input and the output energy spectrum for particles on the energy shell in the Fermi sea shall give the same two-body interaction energy.

The three-body contribution to the binding energy is estimated separately by methods originally developed for nuclear-matter calculations by Bethe and collaborators. Only the S-wave is properly taken into account. Third-order diagrams are also estimated separately.

For the Yntema-Schneider potential given by Brueckner and Gammel, we obtain a total binding energy for liquid  $^3\text{He}$  of  $-1.0^\circ\text{K}$  per particle, which is in general agreement with other calculations. For the Frost-Musulin potential given by Bruch and McGee, we get  $-2.0^\circ\text{K}$  per particle, which is closer to the experimental value.

Also, other low-temperature properties, such as the compressibility, the coefficient of thermal expansion, and the magnetic susceptibility, are estimated, with results in fair agreement with experimental values. The theoretical results are: 4.3% per atmosphere for the compressibility,  $-0.10T$  ( $^\circ\text{K}$ )<sup>-1</sup> ( $T$  in  $^\circ\text{K}$ ) for the coefficient of thermal expansion, and  $\approx 10$  for the magnetic susceptibility ratio. The quasiparticle effective mass, or equivalently the linear term in the temperature dependence of the specific heat, cannot be estimated very well with our methods.

### I. INTRODUCTION

The first serious attempt to calculate properties of liquid  $^3\text{He}$  at zero temperature by application of a microscopic theory was made by Brueckner and Gammel.<sup>1</sup> The physical basis of the Brueckner theory is the assumption that when two atoms interact, they interact strongly, but at the same time the liquid is so dilute that their interaction with other particles can be treated in an average way. Brueckner and others have developed a method to handle the strong repulsion in the two-body potential. Starting from a perturbation expansion for the energy, the expansion in terms of the large matrix elements of the potential is rearranged and replaced by an expansion in reaction matrix elements. This reaction matrix,  $G$ , is obtained by solution of a two-body problem in the medium.

To include the effects of the Pauli exclusion principle and single-particle energy spectrum, arising from the average interaction of each atom with the medium, Brueckner and Gammel use a Green's function method to obtain a  $G$ -matrix propagator in coordinate space. In the integral equation for the  $G$  matrix, single-particle potentials given by sums of diagonal  $G$ -matrix elements are included in the energy denominator, which introduces a problem of self-consistency. It seems, however, that Brueckner and Gammel treated the single-particle potential energies in intermediate states somewhat arbitrarily in practice, and did not actually maintain the self-consistency of their theoretical prescription. It is therefore important to redo the calculations in a more consistent way. Also, the

method itself can be modified and simplified, and supplemented by calculations of the three-body contribution to the binding energy.

The quantitative agreement with experiment of the results of Brueckner and Gammel<sup>1</sup> is not quite satisfactory, especially for the binding energy and the specific heat. They get a binding energy of  $-0.96^\circ\text{K}$  per particle at a saturation distance of  $2.60 \text{ \AA}$ . This equilibrium spacing is not so far from the observed value of  $2.43 \text{ \AA}$ ,<sup>2</sup> but the binding energy is less than 40% of the experimental value of  $-2.5^\circ\text{K}$  per particle.<sup>3</sup> The effective mass or specific-heat ratio is estimated to be 1.84, while the experimental value is now taken to be 3.08.<sup>4</sup>

The compressibility of liquid  $^3\text{He}$  is estimated to be 5.3% per atmosphere and the coefficient of thermal expansion to be<sup>5</sup>  $-0.076T$  ( $^\circ\text{K}$ )<sup>-1</sup> ( $T$  in  $^\circ\text{K}$ ), which are in semiquantitative agreement with experimental results, of which the most recent values are<sup>6</sup> 3.8% per atmosphere and  $-0.14T$  ( $^\circ\text{K}$ )<sup>-1</sup>. The magnetic susceptibility, which is inversely proportional to the energy required to polarize the spins, is calculated, as a ratio to the spin polarization energy of the ideal Fermi gas, to be 12. This is fairly close to the experimental value of 9.<sup>7</sup>

However, as we shall see, we have specific criticisms and modifications to make, so it seems important to redo all the above calculations and estimates in a more consistent way to get a better check on the theory or the potential. The two-body interaction energy contribution to the binding energy of liquid  $^3\text{He}$  has been calculated by the author in

an earlier paper.<sup>8</sup> Later the three-body potential energy contribution to the binding energy was calculated<sup>9</sup> by methods originally developed by Bethe and collaborators for nuclear-matter calculations. Here we will give a summary of calculations of the binding energy, and also try to estimate other properties at zero temperature.

A special problem in our calculations is the two-body potential. The potential chosen seems to have a strong influence on the results of the calculations. Potentials with different forms generally give different results, and the value obtained for the binding energy is extremely sensitive to changes in the potential. In particular, the strongly repulsive short-range part of the potential is still not well known, and may cause relatively large errors in the calculations. The attractive long-range part is probably better determined. We look into this problem by recalculating the binding energy, using a more modern potential<sup>10</sup> than the one which Brueckner and Gammel used.

## 2. BINDING ENERGY

Calculation of the two-body interaction energy contribution to the binding energy has been explained in an earlier paper,<sup>8</sup> which we refer to as I. The calculations were done for two different densities or Fermi momenta  $k_F$ . Here we extend these calculations to other densities because we want to estimate the density-dependence of the binding energy. Then we can find the density at which the energy is a minimum, and can also estimate other properties such as the compressibility, magnetic susceptibility, and coefficient of thermal expansion. Our two-body calculations proceed exactly as explained in I, and results are shown in Table I. The corresponding Table X in I and Table IV in II (see below) are wrong, mainly because of an error by a factor of 2 in Eq. (2.17) in I if the definition (3.31) in I is used.

Calculation of the three-body contribution to the binding energy has been explained in a second paper,<sup>9</sup> which we refer to as II. We also extend these calculations to other densities, and results are shown in Table II for the Kirson method as explained in II.

If, in our two-body calculations, we choose the intermediate-state single-particle potentials equal to zero as in I, and require that the binding energy calculated from our input hole-energy spectrum be equal to the binding energy given by the output G-matrix elements, we get self-consistent solutions for a certain value of the input parameter  $\Delta$  when the other parameter  $m_0^*$  is fixed. The three-body contribution for these parameter values can then be obtained as explained in II, i. e., by interpolations and corrections, and weightings of the results by Fourier transforms of the defect wave function, integrated over intermediate-state momenta. We find that

$$W_3 = \kappa_0^{-1} (2/\pi) \int F_0^2(k) W_3(k) dk. \quad (2.1)$$

Here  $\kappa_0$  is the volume of the correlation hole or the convergence parameter defined in II as

TABLE I. Binding energy for liquid <sup>3</sup>He in °K. Only two-body terms included. Yntema-Schneider potential.  $k_F$  and  $\Delta$  are varied.  $m_0^* = 2.5$ .

$k_F$ (Å <sup>-1</sup> )	0.72	0.75	0.78	0.80
$\Delta$				
0.3	-0.07	0.14	0.48	0.78
0.4	0.33	0.64	1.09	1.49

$$\kappa_0 = \int_0^\infty (\chi_0/k_0)^2 dr = (2/\pi) \int_{k_F}^\infty F_0^2(k) dk, \quad (2.2)$$

and  $F_0(k)$  is the Fourier transform of the partial defect wave function  $\eta$  or  $\chi_0$ , i. e.,

$$F_0(k) = k_0^{-1} \int \mathcal{G}_0(k_0 r) \chi_0(k_0, r) dr, \quad (2.3)$$

or

$$F_0(k) = [Q(P, k) m^* / (\gamma^2 + k^2)] k_0^{-1} \times \int_0^\infty \mathcal{G}_0(k r) v(r) u_L(k_0, r) dr, \quad (2.4)$$

where  $Q(P, k)$  is the Pauli exclusion operator. Details about parameters and wave functions are given in I.

The final results of our calculations are given in Table III together with some corresponding parameter values. The average kinetic energy per particle is

$$T_F = \frac{3}{10} (\hbar^2/M) k_F^2, \quad (2.5)$$

where the Fermi momentum  $k_F$  is related to the density  $\rho$  by

$$\rho = \frac{1}{3} k_F^3 / \pi^2, \quad (2.6)$$

which gives the number of states in the Fermi sea. We also define a mean interparticle spacing  $r_0$  by

$$\rho^{-1} = \frac{4}{3} \pi r_0^3. \quad (2.7)$$

Figure 1 shows the total binding energy  $B$  as a function of the mean radius  $r_0$ . The potential we have used is an Yntema-Schneider potential<sup>11</sup> defined by Brueckner and Gammel as

TABLE II. Three-body energy terms for liquid <sup>3</sup>He in °K. Yntema-Schneider potential.  $k_0 = 0.55 k_F$  on the energy shell.  $k_0$  is varied off the energy shell.  $m_0^* = 2.5$ .

$k_F$ (Å <sup>-1</sup> )	$\Delta$	$m_0^*$	$k_0/k_F$		
			0.6	0.8	1.0
0.72	0.5	2.5	-1.19	-1.31	-1.38
	0.4	2.5	-1.60	-1.81	-1.76
0.75	0.5	1.5	-1.51	-1.71	-1.67
	0.5	2.5	-1.50	-1.70	-1.66
0.78	0.4	2.5	-1.96	-2.29	-1.98
	0.5	1.5	-1.83	-2.15	-1.85
0.80	0.4	2.5	-2.23	-2.51	-2.13

TABLE III. Binding energy for liquid  $^3\text{He}$  in  $^\circ\text{K}$ . Yntema-Schneider potential.  $W_N$  is the interaction energy from the  $N$ -body term,  $E_B$  is the binding energy with only two-body terms included, and  $B_E$  is the total binding energy.  $m_0^* = 2.5$ .

$k_F (\text{\AA}^{-1})$	$r_0 (\text{\AA})$	$\rho (\text{\AA}^{-3})$	$\Delta$	$W_2 (^\circ\text{K})$	$T (^\circ\text{K})$	$E_B (^\circ\text{K})$	$W_3 (^\circ\text{K})$	$B_E (^\circ\text{K})$
0.72	2.67	0.0126	0.37	-2.45	2.55	0.10	-1.00	-0.90
0.75	2.56	0.0142	0.34	-2.50	2.75	0.25	-1.25	-1.00
0.78	2.46	0.0160	0.31	-2.55	3.00	0.45	-1.45	-1.00
0.80	2.40	0.0173	0.29	-2.55	3.15	0.60	-1.55	-0.95

$$V_{\text{YS}}(r) = 7250(1200 e^{-4.82r} - 1.24/r^6 - 1.89/r^8), \quad (2.8)$$

in  $^\circ\text{K}$ , where  $r$  is measured in angstroms.

From Fig. 1 we get an energy minimum of  $-1.02^\circ\text{K}$  per particle for  $r_0 = 2.51 \text{ \AA}$  or  $k_F = 0.765 \text{ \AA}^{-1}$ . The corresponding experimental values are  $-2.5^\circ\text{K}$  per particle<sup>3</sup> for the binding energy, and  $2.43 \text{ \AA}$  or  $0.79 \text{ \AA}^{-1}$  for the density parameters, obtained from the molar volume.<sup>2, 6, 12</sup> Other calculated values for the binding energy are Beck's  $+1.51^\circ\text{K}$  per particle,<sup>13</sup> Brueckner and Gammel's  $-0.96^\circ\text{K}$  per particle,<sup>1</sup> Beck and Sessler's  $-1.16^\circ\text{K}$  per particle,<sup>14</sup> Woo's  $-1.35^\circ\text{K}$  per particle,<sup>15</sup> and Schiff and Verlet's  $-1.35^\circ\text{K}$  per particle.<sup>16</sup> According to Massey and Woo,<sup>17</sup> a second-order perturbation correction can be added to the result of Schiff and Verlet to give approximately  $-1.6^\circ\text{K}$  per particle.

### 3. THIRD-ORDER DIAGRAMS

A rearranged low-density expansion may be expected to converge fairly rapidly in nuclear matter, and perhaps also in liquid  $^3\text{He}$ . The approximate methods applied are based on a selective summation of certain classes of terms in the general perturbation expansion. The types of diagrams which are included are generally particle-particle ladder diagrams with self-energy insertions.

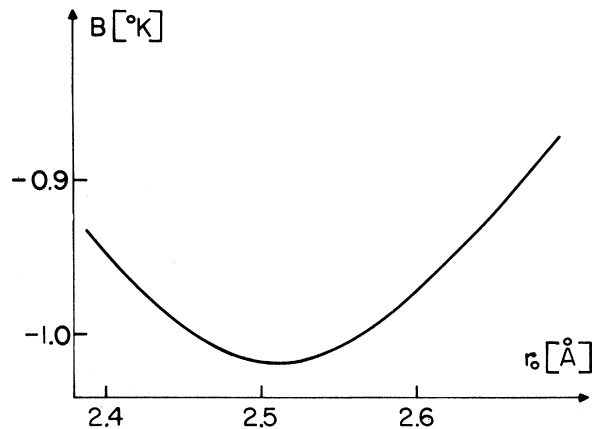


FIG. 1. Binding energy  $B$  for liquid  $^3\text{He}$  as a function of mean interparticle spacing  $r_0$ . Yntema-Schneider potential.  $m_0^* = 2.5$ .

In nuclear-matter calculations, ring diagrams like Fig. 2 are usually not included because they would give a relatively small correction to the energy of the system. These ring diagrams are probably more important for liquid  $^3\text{He}$ .

Additional cluster diagrams are generally not included in the calculations. They represent diagrams topologically different from the ladder diagrams, self-energy insertions, and ring diagrams. These diagrams represent effects of clusters of more than two particles, which should be important only in rather dense fluids. They can probably be neglected in calculations for nuclear matter, but for liquid  $^3\text{He}$  the validity of such a neglect is not obvious. The diagrams with three hole lines are, however, included in the three-body calculations.

We can assume that diagrams involving diagonal  $G$ -matrix elements are generally larger than those involving off-diagonal ones. This assumption is supported by the calculations of nondiagonal  $G$ -matrix elements in I. The usual diagonal form occurs in bubble insertions. In principle, these bubble-insertions can be included in the single-particle energies, or they can be estimated by separate calculations.

The contribution of all three-body diagrams can be evaluated by the methods applied in II. These methods were developed for nuclear-matter calculations, and are not necessarily so convincing for liquid  $^3\text{He}$ , where not only the  $S$ -wave, but also higher partial waves are potentially important. Also, typical hole momenta are not so small compared to the inverse range of the strong repulsion in liquid  $^3\text{He}$ , as in nuclear matter. It would be very complicated, however, to develop present methods further to take this into account. According to Kirson,<sup>18</sup> it is a very good approximation to include only  $S$ -wave terms. The main justification for neglecting higher partial waves

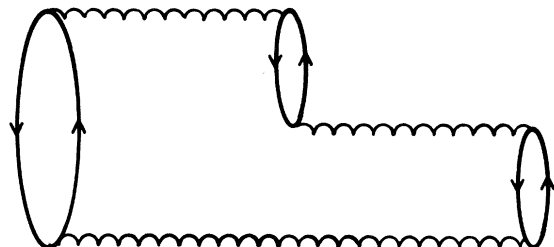


FIG. 2. Third-order ring diagram.

is that averaging over hole momenta and integration over directions of momenta eliminates higher partial waves and leaves only the  $S$ -wave parts. We assume that the ratio between two  $S$  waves is a good approximation for the ratio between total wave functions; for instance, that the effective interaction can be written as

$$g_L(r) = v(r)u_L(k_0, r)/g_L(k_0 r) \approx v(r)u_0(k_0, r)/g_0(k_0 r) \quad (3.1)$$

for all  $L$ . According to Figs. 7 and 8 in I, this approximation should be fair enough for the lower partial waves.

Nonetheless, one should try to check the final results in II. The only diagonal matrix elements in the three-body diagrams are the particle-bubble and the hole-bubble diagrams, which are shown in Fig. 3. These bubble diagrams are larger than any three-body diagram involving an off-diagonal matrix element. Thus, bubble diagrams of third order with one interaction in the middle should dominate the effects of the three-body clusters.

We can estimate these diagrams crudely in the following way. The effect of two  $(Q/e)g$  factors can be expressed approximately by the pair excitation probability  $\kappa$  defined by

$$\kappa = 4\pi\rho \left[ \frac{1}{4} \sum_{\text{even } L} + \frac{3}{4} \sum_{\text{odd } L} \right] (2L+1) \int_0^\infty (\chi_L/k_0)^2 dr = \pi\rho \sum_L \kappa_L \quad (3.2)$$

The three-body function  $F(r)$  defined by Eq. (3.19) in II, should in fact approach asymptotically the value

$$F(\infty) \approx 4\pi\kappa_0 \quad (3.3)$$

where  $\kappa_0$  is defined by Eq. (2.2), i. e., by Eq. (3.2) for  $L=0$ .

Summing over hole states, and including exchange terms, we get roughly

$$W_3 \approx 2\kappa W_2 \approx \frac{1}{2}\kappa\rho G, \quad (3.4)$$

where  $G$  is taken for some average momentum, on the energy shell for the hole-bubble diagram.

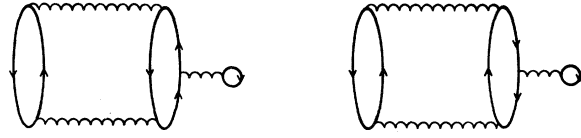


FIG. 3. Third-order particle-bubble and hole-bubble diagrams, i. e., diagrams with diagonal  $G$ -matrix elements.

This approximation would probably be all right as a rough estimate for the three-body energy, except when all three particles are in relative  $S$  waves. Then one must include rescattering effects as in the calculations of II.

The results are shown in Table IV. The relative momentum  $k_0$  is chosen to be the same on and off the energy shell and for all partial waves, and is  $k_0 = 0.55k_F$ .

The bubble diagrams can also be estimated roughly by treating each partial wave separately in the expression for  $\kappa$ . From the Tables XI and XII in I, we see that most of the contribution to  $\kappa$  comes from the partial waves for  $L=0$  and  $L=1$ , so we can neglect higher values of  $L$ .

The values of  $\kappa$  are taken from the Tables XI and XII in I for  $k_0 = 0.55k_F$ . The corresponding  $G$ -matrix elements have to be taken at different average momenta, since, as may be seen from Figs. 9 and 10 in I, the Fourier transform  $F_0(k)$  peaks at  $k \approx k_F$  and  $F_1(k)$  at  $k \approx 1.6k_F$ . The corresponding relative momenta are  $k_0 = 0.5k_F$  for  $L=0$  and  $k_0 = 0.8k_F$  for  $L=1$ . Equation (3.4) can then be written as

$$W_3 \approx \frac{1}{2} [\kappa_0 \rho G(0.5k_F) + \kappa_1 \rho G(0.8k_F)], \quad (3.5)$$

which should reproduce the diagrams in Fig. 3. The results are given in Table V.

In our general calculations, the single-particle energies of the holes are chosen to cancel bubble diagrams as indicated by Fig. 4, so we can forget about the hole-bubble diagram in Fig. 3. The particle-bubble diagram could be estimated by means of Eq. (3.4) with  $G$  taken off the energy shell, but the direct matrix elements are not the only large ones. The corresponding exchanges

TABLE IV. Three-body energy contributions from hole-bubble and particle-bubble diagrams, defined by Eq. (3.4). Yntema-Schneider potential.  $G$  (on) or  $G$  (off) are diagonal matrix elements in Å, calculated on or off the energy shell.  $W_3$  is the energy contribution in °K.  $\Delta$  and  $m_0^*$  are varied.

$k_0/k_F$	$k_F$ (Å <sup>-1</sup> )	$\Delta$	$m_0^*$	$\kappa$	$G$ (on)	$G$ (off)	Hole bubble	$W_3$	Particle Bubble
0.55	0.75	0.4	2.5	0.267	-44.5	-22.0	-1.38	-0.68	
		0.5	1.5	0.262	-39.5	-10.0	-1.20	-0.30	
	0.78	0.4	2.5	0.306	-37.5	-12.5	-1.50	-0.50	
		0.5	1.5	0.301	-32.0	0.5	-1.26	0.02	
	0.75	0.4	2.5	0.267	-24.5	51.5	-0.76	1.59	
		0.5	1.5	0.262	-23.5	64.0	-0.71	1.94	
0.80	0.4	2.5	0.306	-13.5	70.5	-0.54	2.82		
	0.78	0.5	1.5	0.301	-12.0	84.0	-0.47	3.30	

TABLE V. Three-body energy terms from bubble diagrams for liquid  $^3\text{He}$ , estimated according to Eq. (3.5). Yntema-Schneider potential.  $G(k_0)$  are diagonal matrix elements in  $\text{\AA}$ , and  $W_3$  is the three-body potential energy contribution in  $^\circ\text{K}$ .  $\Delta$  and  $m_0^*$  are varied.

$k_F(\text{\AA}^{-1})$	$\Delta$	$m_0^*$	$\kappa_0$	$\kappa_1$	$G(0.5k_F)$	$G(0.8k_F)$	$W_3$		Total
							$L=0$	$L=1$	
$\langle k_0   G   k_0 \rangle$ calculated on the energy shell									
0.75	0.4	2.5	0.188	0.076	-44.6	-24.5	-0.97	-0.22	-1.19
	0.5	1.5	0.185	0.075	-39.1	-23.5	-0.84	-0.20	-1.04
0.78	0.4	2.5	0.212	0.091	-38.3	-13.5	-1.06	-0.16	-1.22
	0.5	1.5	0.208	0.090	-32.3	-12.0	-0.88	-0.14	-1.02
$\langle k_0   G   k_0 \rangle$ calculated off the energy shell									
0.75	0.4	2.5	0.188	0.076	-30.4	51.5	-0.66	0.45	-0.21
	0.5	1.5	0.185	0.075	-18.6	64.0	-0.40	0.56	0.16
0.78	0.4	2.5	0.212	0.091	-22.6	70.5	-0.63	0.84	0.21
	0.5	1.5	0.208	0.090	-9.6	84.0	-0.26	0.99	0.73

are also large. Hence we estimate the contribution of several third-order diagrams in the following way.

The direct diagrams in Fig. 5 have a particle-hole interaction in the middle. The most important difference between the bubble diagram and the other third-order diagrams is that the bubble interaction is diagonal, while the latter have nondiagonal interactions in the middle. But in all three diagrams in Fig. 5, the momentum is changed only slightly or not at all by the middle interaction, and the value of the matrix element is not affected much by this small change. Therefore the three diagrams are approximately equal, except for the statistical weight factors, and their sum is then approximately zero.

Similarly, the exchange diagrams in Fig. 6 all involve large momentum change in the middle interaction, and these momentum changes are about equal. Then the sum of these diagrams, with statistical weights included, is approximately equal to zero.

In the same way, the third-order diagrams shown in Figs. 7 and 8 roughly cancel each other. These diagrams have an additional weight of  $-\frac{1}{2}$  relatively to the diagrams in Figs. 5 and 6. The final conclusion is that it does not help anything to estimate the third-order particle-bubble diagram or ring diagram, because exchange diagrams roughly cancel these diagrams. This should be valid at least for the higher partial waves, i.e., for  $L > 1$ ; for  $L = 0$  we have the exact calculations by our Kirson method.

The hole-hole and hole-bubble interactions, which are not considered above, can in principle

be absorbed in the hole potential energy as already mentioned, and then the three-body energy contribution may be rather small because of cancelling statistical effects among the third-order diagrams. We will, however, estimate the third-order hole-hole diagram which is shown in Fig. 9, since this diagram is not really included in our earlier calculations. This diagram can be estimated in the same way as the hole-bubble diagram, i.e., by Eq. (3.4) with  $G$  taken on the energy shell. But because of extra limitations on the hole momenta in the Fermi sea, and because the diagram is symmetric, we get a total relative weight of  $\frac{1}{16}$  compared with the direct hole-bubble diagram. Using results from II in Eq. (3.4), we finally get an energy contribution of  $-0.1^\circ\text{K}$  from this diagram. Adding this energy to the binding energy obtained, we get a total binding energy of  $-1.0^\circ\text{K}$  per particle, as shown in Table III and Fig. 1.

The hole-hole scattering corrections are probably not important for calculations of the total energy. But they introduce more important corrections into the single-particle energies, particularly near the Fermi surface. And inclusion of particle-hole scattering could make a significant contribution to the energy also.

#### 4. EFFECT OF EXCLUSION PRINCIPLE

In Brueckner's theory, the Pauli exclusion principle limits the number of states available for the two atoms being considered. To include the effects of the exclusion principle and the single-particle energy spectrum, a Green's func-

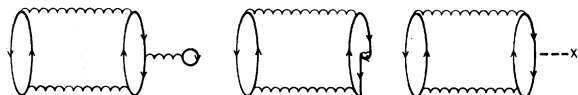


FIG. 4. Third-order diagrams, cancelling each other to define the single-particle energy spectrum for holes.

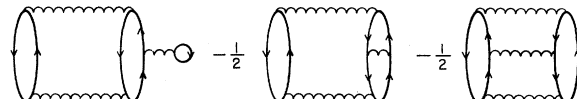


FIG. 5. Direct third-order diagrams with relative weights.

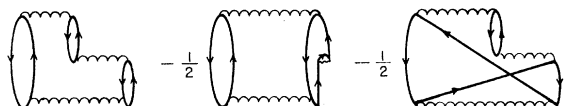


FIG. 6. Exchange third-order diagrams with relative weights.

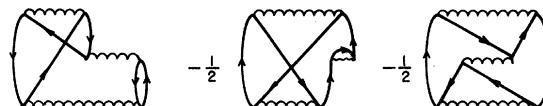


FIG. 8. Some third-order diagrams with relative weights.

tion method is used to evaluate a  $G$ -matrix propagator in coordinate space, as outlined in I. For nuclear matter, Bethe *et al.*,<sup>19</sup> have developed a method to calculate a relatively simple reference reaction matrix, in which the exclusion principle is neglected in some way in first approximation, i. e., the Pauli exclusion operator is set equal to one. This method could possibly be applied to liquid <sup>3</sup>He too, if the exclusion principle were not too important, and did not change results too much.

The exclusion principle should have some effect on the results of the calculations. For slow particles, the exclusion principle increases the contribution from the strongly repulsive core quite a lot. This effect decreases as the Fermi surface is approached, and the interaction energy becomes more negative. The variation of the effect of the exclusion principle on particles moving at different depths in the Fermi sea thus gives a variation in the single-particle potential. Also, a more rapidly moving particle excites the higher states of relative angular momentum more strongly when it collides with other particles in the medium.

To estimate the importance of including the exclusion principle, we have calculated the main first-order term in the original reference spectrum method of Bethe *et al.*,<sup>19</sup> which we denote as the RS method, using the same input energy spectrum as in our other two-body calculations which are performed with what we denote as the BG method. That is, we have neglected the exclusion principle and used Eq. (3.38) in I instead of Eq. (3.36) for the Green's functions  $\Gamma_L(r, r')$  in I, when solving the Bethe-Goldstone equation.<sup>20</sup> Results for the two methods are compared in Tables VI and VII for some typical standard parameter values. The  $G$ -matrix elements are given in  $\text{\AA}$ , which can be converted to ( $^\circ\text{K \AA}^3$ ), the conversion factor being

$$\hbar^2/M = 16.36^\circ\text{K \AA}^2. \quad (4.1)$$

From these tables it seems obvious that the exclusion principle cannot be neglected as a first approximation, at least not for the S wave. For higher partial waves, the approximation is not too bad, at least for  $L > 1$ . So one could possibly use

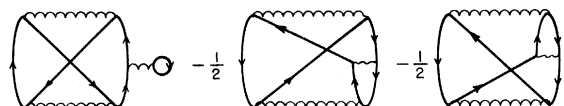


FIG. 7. Some third-order diagrams with relative weights.

a procedure in which the exclusion principle is included for  $L=0$  and  $L=1$ , and neglected for  $L=2$  and  $L=3$ . For  $L > 3$ , one can just replace the  $G$  matrix by the two-body potential, or the perturbed wave function by the unperturbed one, as explained in I.

### 5. SPECIFIC HEAT AND COMPRESSIBILITY

In addition to the binding energy, we also would like to estimate theoretical values for other properties such as the compressibility, the magnetic susceptibility, and the coefficient of thermal expansion. All these properties can be calculated from our  $G$ -matrix elements, but complications arise because the  $G$  matrix is density dependent. We get the so-called rearrangement energy in addition to the usual potential energy term.

If we write  $n_i$  for the occupation number of the state  $i$ , i. e.,

$$\begin{aligned} n_i &= 1 \text{ for } k_i < k_F, \\ &= 0 \text{ for } k_i > k_F, \end{aligned} \quad (5.1)$$

and  $\rho^{(+)}$  and  $\rho^{(-)}$  for the densities of atoms with spin up and spin down respectively, then the total ground-state energy for

$$\rho^{(+)} = \rho^{(-)} = \frac{1}{2}\rho \quad (5.2)$$

can be written

$$\begin{aligned} E(\rho^{(\pm)}) &= \frac{1}{2} \sum_i n_i \hbar^2 k_i^2 / M \\ &+ \frac{1}{2} \sum_{i,j} n_i n_j [\langle \vec{k}_{ij} | G(\rho) | \vec{k}_{ij} \rangle - \text{exchange}]. \end{aligned} \quad (5.3)$$

Brueckner writes the energy of a quasiparticle with spin up in the unpolarized medium as

$$\epsilon_i^{(+)} = \delta E / \delta n_i^{(+)} = \frac{1}{2} \hbar^2 k_i^2 / M + U(k_i) + U_R, \quad (5.4)$$

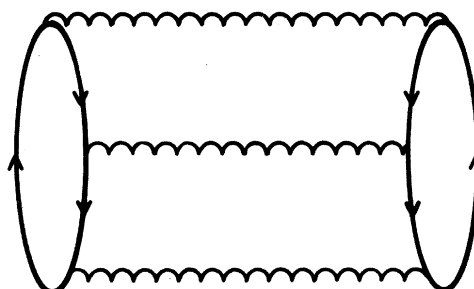


FIG. 9. Third-order hole-hole diagram.

TABLE VI. Diagonal  $G_L$ -matrix elements in  $\text{\AA}$ , calculated on the energy shell. Statistical weights are included. BG method is with the exclusion principle included; RS method is with the exclusion principle neglected. Yntema-Schneider potential.  $k_0$  is varied.  $k_F = 0.75 \text{\AA}^{-1}$ .  $\Delta = 0.5$ .  $m_0 = 2.5$ .

Method	$k_0/k_F$	$L=0$	$L=1$	$L=2$	$L=3$	$L>3$	Total
BG	0.125	16.5	-12.1	-0.1	0	0	4.2
	0.25	27.4	-38.8	-1.3	-0.3	0	-13.1
	0.375	40.1	-61.8	-4.7	-1.9	-0.4	-28.7
	0.50	51.0	-69.9	-9.6	-6.2	-1.7	-36.4
	0.625	58.0	-60.3	-15.0	-12.9	-3.7	-33.9
	0.75	60.5	-34.5	-19.8	-21.5	-6.7	-22.0
	0.875	58.6	3.1	-22.9	-31.8	-10.9	-4.0
	1.00	53.1	45.9	-23.3	-43.3	-16.5	16.0
RS	0.125	-2.8	-12.5	-0.1	0	0	-15.4
	0.25	7.9	-40.0	-1.4	-0.3	0	-33.7
	0.375	20.2	-63.8	-4.8	-1.9	-0.4	-50.8
	0.50	30.3	-72.3	-9.8	-6.3	-1.7	-59.7
	0.625	36.4	-62.5	-15.4	-13.0	-3.7	-58.1
	0.75	37.9	-35.9	-20.4	-21.7	-6.7	-46.8
	0.875	35.2	2.5	-23.7	-32.1	-10.9	-29.1
	1.00	29.2	45.4	-24.1	-43.7	-16.5	-9.8

where the single-particle potential  $U(k_i)$  is

$$U(k_i) = \sum_j n_j \langle \vec{k}_{ij} | G(\rho) | \vec{k}_{ij} \rangle. \quad (5.5)$$

The last term in Eq. (5.4) is

$$U_R = \frac{1}{2} \Omega^{-1} \sum_{j,k} n_j n_k \times \left( \frac{\partial \langle \vec{k}_{jk} | G(\rho^{(+)}, \rho^{(-)}) | \vec{k}_{jk} \rangle}{\partial \rho^{(+)}} \right) \rho^{(+)} = \rho^{(-)} = \frac{1}{2} \rho, \quad (5.6)$$

which is the rearrangement energy and arises

from the density dependence of the  $G$  matrix. It follows from the relations

$$\partial G(\rho) / \partial n_i = [\partial G(\rho) / \partial \rho] / (\partial \rho / \partial n_i), \quad (5.7)$$

$$\text{and } \rho = \sum_i (n_i / \Omega), \quad (5.8)$$

which is just Eq. (2.6). The rearrangement energy represents the difference between the energy required to remove a particle quickly to infinity with no change in the states of the rest of the system, and the energy required to remove the particle adiabatically to infinity with the rest of the system

TABLE VII. Diagonal  $G_L$ -matrix elements in  $\text{\AA}$ , calculated on the energy shell. Statistical weights included. BG method is with the exclusion principle included; RS method is with the exclusion principle neglected. Yntema-Schneider potential.  $k_0$  is varied.  $k_F = 0.78 \text{\AA}^{-1}$ .  $\Delta = 0.5$ .  $m_0^* = 2.5$ .

Method	$k_0/k_F$	$L=0$	$L=1$	$L=2$	$L=3$	$L>3$	Total
BG	0.125	24.1	-13.0	-0.1	0	0	11.0
	0.25	35.6	-40.8	-1.5	-0.3	-0.1	-7.1
	0.375	48.5	-63.2	-5.2	-2.3	-0.6	-22.7
	0.50	58.9	-68.7	-10.4	-7.2	-1.9	-29.3
	0.625	64.9	-55.1	-15.9	-14.5	-4.2	-24.7
	0.75	66.0	-24.6	-20.6	-23.7	-7.6	-10.6
	0.875	62.4	17.1	-23.1	-34.9	-12.3	9.3
	1.00	55.3	62.5	-22.4	-46.7	-18.6	30.2
RS	0.125	-0.3	-13.3	-0.1	0	0	-13.7
	0.25	11.0	-41.9	-1.5	-0.3	-0.1	-32.9
	0.375	23.6	-65.1	-5.3	-2.3	-0.6	-49.7
	0.50	33.5	-70.9	-10.7	-7.2	-1.9	-57.2
	0.625	38.9	-56.9	-16.4	-14.6	-4.2	-53.2
	0.75	39.3	-25.6	-21.3	-24.0	-7.6	-39.2
	0.875	35.4	16.6	-24.0	-35.3	-12.3	-19.6
	1.00	28.4	61.3	-23.3	-47.2	-18.6	0.7

rearranging itself to the new ground state.

The Hugenholtz-Van Hove theorem<sup>21</sup> states that the energy of a particle on the Fermi surface is equal to the negative of the energy required to remove the particle adiabatically to infinity, i. e., the separation energy; and it is equal to the average energy of all the particles in the system. Then the separation energy is the negative of the energy which the system acquires when one particle is added at constant volume, while the average energy is the energy acquired when a single particle is added at constant density. The Hugenholtz-Van Hove theorem is, however, not directly applicable to reaction-matrix calculations.<sup>22</sup> It is strictly valid only if the single-particle energy spectrum is continuous at the Fermi surface. But some single-particle energies should in principle be calculated off the energy shell, and the rearrangement energy is usually neglected in calculations of the binding energy where we have a gap in the single-particle spectrum at the Fermi surface.

For momenta near the Fermi surface, we can rewrite Eq. (5.4) in the form

$$\epsilon_i^{(+)} = \frac{1}{2} \hbar^2 k_i^2 / M^* + \text{constant}, \quad (5.9)$$

with

$$1/M^* = 1/M + [\partial U(k)/\partial k]_{k=k_F} / (\hbar^2 k_F). \quad (5.10)$$

Close to zero temperature, the specific heat is mainly determined by the single-particle level density near the Fermi surface. The anomaly in the level density is described by the concept of the effective mass  $M^*$  or the corresponding dimensionless quantity  $m^*$ . We write the excitation energy (5.4) or (5.9) near the Fermi surface as

$$\epsilon(k) = \frac{1}{2} (\hbar^2/M) k^2 + U(k) = \frac{1}{2} (\hbar^2/M^*) k^2 + U(k_F), \quad (5.11)$$

where

$$1/m^* = M/M^* = 1 + (M/\hbar^2) [\partial U(k)/\partial k]_{k=k_F} / k_F. \quad (5.12)$$

The specific heat at zero temperature is then determined by the single-particle energy spectrum (5.11), and the variation is proportional to the variation or change in the level density, i. e.,

$$C/C_F = M^*/M = m^*, \quad (5.13)$$

where  $C_F$  is the specific heat of an ideal Fermi gas. The calculations of Brueckner and Gammel predict that the specific heat near absolute zero temperature should increase if the liquid is compressed, but their estimated value for  $m^*$  at equilibrium density is 1.84, while the experimental value is 3.08.<sup>6</sup> It is, however, probably unfair to compare these two results directly because of the gap in the single-particle spectrum at the Fermi surface in the BG method.

We have not tried to calculate any effective mass from our results, because we used rather different input particle and hole energy spectra near the

Fermi momentum, and because we have set the center-of-mass momentum equal to zero. The last approximation affects the slope of our output single-particle spectrum, especially at the Fermi surface. Also, the three-body energy is not included when the output single-particle energies are calculated. So we have just used the value  $m_0^* = 2.5$  as a parameter in our input energy spectrum for the hole states.

The on-energy-shell single-particle energy spectrum could probably in principle both satisfy the Hugenholtz-Van Hove theorem and give the correct effective mass or specific heat, while the off-energy-shell spectrum corresponds to free propagation for large excitation energies. But it would be very complicated to make a completely self-consistent version of Brueckner theory, satisfying these criteria and including both the two-body- and the three-body potential energy.

It is possible to obtain an approximate value for the compressibility from our calculations. Liquid <sup>3</sup>He has a remarkably high compressibility which is qualitatively what one expects for a low-density system, and it would be interesting if we could reproduce this value.

The compressibility coefficient is given by

$$\beta = - \frac{(\partial \Omega / \partial \mathcal{P})_T}{\Omega} = \frac{1/\rho}{\partial \mathcal{P} / \partial \rho} = \frac{3/k_F}{\partial \mathcal{P} / \partial k_F}, \quad (5.14)$$

where  $\mathcal{P}$  is the pressure

$$\mathcal{P} = - \frac{\partial E}{\partial \Omega} = \frac{\rho^2}{N} \frac{\partial E}{\partial \rho} = \frac{1}{3} \rho k_F \frac{(\partial E / \partial k_F)}{N}. \quad (5.15)$$

If we assume a quadratic dependence of the energy on density, we can write

$$E - E_0 = A(\rho - \rho_0)^2 = \Delta E, \quad (5.16)$$

$$\partial E / \partial \rho = 2A(\rho - \rho_0) = 2A(\Delta \rho),$$

where  $E_0$  and  $\rho_0$  are the minimum binding energy and the equilibrium density, given by Fig. 1. Figure 1 shows that the energy rises by 0.02°K per particle when  $r_0$  decreases from 2.51 to 2.46 Å, i. e., when the density  $\rho$  increases from 0.0151 to 0.0160 Å<sup>-3</sup>. This gives us the constant  $A$ , i. e.,

$$A = (\Delta E) / (\Delta \rho)^2, \quad (5.17)$$

and we can write the pressure-density relation (5.15) as

$$\mathcal{P} = \beta^{-1} (\rho / \rho_0 - 1), \quad (5.18)$$

where

$$\beta^{-1} = 2K\rho_0^3 \Delta E / (\Delta \rho)^2 = 23.2 \text{ atm.} \quad (5.19)$$

Here  $K$  is Boltzmann's constant, and we get a volume change of



$$\beta = 4.3\% \text{ per atm.} \quad (5.20)$$

The experimental value for  $\beta$  is extrapolated to be 3.8% per atm.<sup>2,6</sup> Brueckner and Gammel<sup>1</sup> give the result of 5.3% per atm. We have, however, been unable to reproduce their result from their given data and in the way they claim the calculation is done. In fact, we have found that their value should be closer to 10% per atm, but of course there may be a misprint or a misunderstanding somewhere. On the other hand, the curve they present for the binding energy as function of the mean interparticle spacing  $r_0$ , is in fact rather flat, which means a large value for  $\beta$  because  $\partial E/\partial \rho$  is then small. Since their equilibrium density is low, one would expect a large compressibility coefficient from their results. Another theoretical result is 9.9% per atm, due to Woo.<sup>15a</sup> The compressibility coefficient, however, depends strongly on density; and at the experimental equilibrium density, with the binding energy fitted to the experimental energy, Woo<sup>15b</sup> obtains 3.6% per atm.

Our result is surprisingly close to experimental values. This, however, should not be taken too seriously, but only as an indication of results which might be expected from more refined calculations.

## 6. THERMAL EXPANSION

The coefficient of thermal expansion,  $\alpha$ , is given by the relation

$$\alpha = (\partial \Omega / \partial T) / \Omega = - (\partial S / \partial \Phi) / \Omega, \quad (6.1)$$

where the first term is valid for constant pressure, i. e., for  $\Phi = 0$  at equilibrium. To estimate  $\alpha$ , we can use the pressure-density relation developed in Sec. 5, but we need an expression for the entropy  $S$ .

The specific heat at constant volume is given by Eq. (5.13), i. e.,

$$C = (M^*/M) C_F, \quad (6.2)$$

where  $C_F$  is the specific heat of the ideal Fermi gas, which is

$$C_F = \frac{1}{2} k_F \frac{M}{\hbar^2} \Omega K^2 T = \left( \frac{1}{3} \pi \right)^{2/3} \frac{M}{\hbar^2} N \left( \frac{\Omega}{N} \right)^{2/3} K^2 T. \quad (6.3)$$

The ratio  $M^*/M$ , which determines the change in level density from that of the ideal Fermi gas, can be estimated as a function of density. Equation (5.12) gives

$$\frac{M^*}{M} = \left( 1 + \frac{M}{\hbar^2} \frac{\partial U / \partial k_F}{k_F} \right)^{-1} = \frac{M_0^*}{M} + B \left( 1 - \frac{\Omega}{\Omega_0} \right), \quad (6.4)$$

where  $M_0^*$  and  $\Omega_0$  are the effective mass and the volume at zero pressure and equilibrium density. Then

$$\Omega_0 = \frac{4}{3} \pi r_0^3 N, \quad (6.5)$$

where our calculations give

$$r_0 = 2.51 \text{ \AA}, \quad (6.6)$$

as indicated by Fig. 1. The constant  $B$  has to be estimated in some way, since we have no curve for the effective mass as function of density.

The entropy is

$$S = \int_0^T dT' C(T') / T' = \frac{1}{3} k_F (M^* / \hbar^2) \Omega K^2 T \\ = \left( \frac{1}{3} \pi \right)^{2/3} (M^* / \hbar^2) N (\Omega / N)^{2/3} K^2 T, \quad (6.7)$$

where a possible variation of  $M^*$  with temperature is neglected. For the pressure-density relation, Eq. (5.18) is written

$$\Phi = \beta^{-1} (1 - \Omega / \Omega_0), \quad (6.8)$$

and using

$$\partial \Omega / \partial \Phi = -\beta \Omega_0, \quad (6.9)$$

we get from Eqs. (6.7) and (6.8) for  $\Omega = \Omega_0$  the expression

$$\alpha = \left( \frac{1}{3} \pi \right)^{2/3} \frac{M}{\hbar^2} N^{1/3} \beta K^2 \left( \frac{\partial}{\partial \Omega} \frac{\Omega^{2/3} M^*}{M} \right)_{\Omega = \Omega_0} \quad (6.10)$$

for Eq. (6.1). Using Eq. (6.4) to obtain  $\partial M^* / \partial \Omega$ , we finally get

$$\alpha = \frac{2}{3} \left( \frac{1}{3} \pi \right)^{2/3} \frac{M}{\hbar^2} \left( \frac{N}{\Omega_0} \right)^{1/3} \beta K^2 T \left( \frac{M_0^*}{M} - \frac{3}{2} B \right). \quad (6.11)$$

If we assume that  $\partial U / \partial k_F$  is proportional to the density  $\rho$  near equilibrium density, which looks like a reasonable assumption from our various calculations, we can write

$$k_F^{-3} \frac{\partial U}{\partial k_F} = \frac{\hbar^2}{M^*} \frac{1 - M^*/M}{k_F^2} = \text{constant}. \quad (6.12)$$

Using the parameter values  $m_0^* = 2.5$  and  $k_F = 0.765 \text{ \AA}^{-1}$  at our equilibrium density, we get the value  $-1.025$  for this constant. Inserted in Eq. (6.4), this gives an effective mass ratio of 2.66 for  $k_F = 0.78 \text{ \AA}^{-1}$ , which leads to  $B = 2.8$ . Finally we obtain from Eq. (6.11)

$$\alpha = -0.10 T \text{ (}^\circ\text{K)}^{-1}. \quad (6.13)$$

The last term with the constant  $B$  in Eq. (6.11) arises from the density variation of the effective mass. We see that this term changes the sign of  $\alpha$ , and if it were neglected, we would get a positive coefficient of thermal expansion and the liquid would contract when cooled near zero temperature.

This anomaly in the coefficient of thermal expansion can be explained by the dominant effects of Fermi statistics at very low temperatures. When the liquid is cooled, the tendency of the <sup>3</sup>He atoms to form a state of momentum order is inhibited by the effects of the strong forces. The repulsion is increased by the exclusion principle in

the degenerate state, while the attraction becomes less effective because of the high zero-point energy and short wavelengths. The liquid consequently expands as the atoms drop down into the states of momentum order.

Brueckner and Atkins<sup>5</sup> obtained the value of  $\alpha = -0.076T$  ( $^{\circ}\text{K}$ )<sup>-1</sup>, which is only in semiquantitative agreement with the latest experimental results. But they used a value of 27.5 atm for the parameter  $\beta^{-1}$  instead of 18.9 atm which Brueckner and Gammel<sup>1</sup> estimated in their calculations. This procedure seems somewhat inconsistent, since other parameters such as  $\Omega_0$  and  $M_0^*$  were taken from the BG calculations. How-

ever, if Brueckner and Atkins had used the other value for  $\beta^{-1}$ , they would have obtained the result of  $\alpha = -0.11T$  ( $^{\circ}\text{K}$ )<sup>-1</sup>, which is much closer to recent experimental values.

Our result (6.13) is in general agreement with experimental results. It can be compared with other values given by various people, such as the  $-0.076T$  ( $^{\circ}\text{K}$ )<sup>-1</sup> of Brueckner and Atkins,<sup>5</sup> the  $-0.08T$  ( $^{\circ}\text{K}$ )<sup>-1</sup> of Anderson *et al.*,<sup>23</sup> the  $-0.103T$  ( $^{\circ}\text{K}$ )<sup>-1</sup> of Goldstein,<sup>24</sup> the  $-0.105T$  ( $^{\circ}\text{K}$ )<sup>-1</sup> of Brewer and Daunt,<sup>25</sup> the  $-0.12T$  ( $^{\circ}\text{K}$ )<sup>-1</sup> of Rives and Meyer,<sup>26</sup> the  $-0.125T$  ( $^{\circ}\text{K}$ )<sup>-1</sup> of Kerr and Taylor,<sup>12</sup> and the  $-0.14T$  ( $^{\circ}\text{K}$ )<sup>-1</sup> of Boghosian *et al.*<sup>6</sup>

## 7. MAGNETIC SUSCEPTIBILITY

The magnetic susceptibility is a measure of the energy required to produce a net spin alignment in a given direction. It is inversely proportional to the energy required to polarize the spins. This energy has been given by Brueckner and Gammel in the limit of small spin alignment as an equation similar to Eq. (5.3). If  $\rho^{(+)}$  and  $\rho^{(-)}$  are the densities of atoms with spin up and spin down respectively, we can write

$$E_{\sigma}(\rho^{(+)}, \rho^{(-)}) = \frac{1}{2} \sum_i n_i \hbar^2 k_i^2 / M + \frac{1}{2} \sum_{i,j} n_i n_j [ \langle \vec{k}_{ij} | G(\rho^{(+)}, \rho^{(-)}) | \vec{k}_{ij} \rangle - \text{exchange} ], \quad (7.1)$$

$$\begin{aligned} \text{where } n_i^{(+)} &= 1 \text{ for } k_i < k_F^{(+)}, & n_i^{(-)} &= 1 \text{ for } k_i < k_F^{(-)}, \\ &= 0 \text{ for } k_i > k_F^{(+)}, & &= 0 \text{ for } k_i > k_F^{(-)}, \end{aligned} \quad (7.2)$$

$$\begin{aligned} \text{and } \sum_i n_i^{(+)} &= \Omega \rho^{(+)} = \Omega (2\pi\hbar)^{-3} \frac{4}{3} \pi \rho_F^{(+)} = \Omega \frac{1}{6} k_F^{(+)}{}^3 / \pi^2, \\ \sum_i n_i^{(-)} &= \Omega \rho^{(-)} = \Omega (2\pi\hbar)^{-3} \frac{4}{3} \pi \rho_F^{(-)} = \Omega \frac{1}{6} k_F^{(-)}{}^3 / \pi^2. \end{aligned} \quad (7.3)$$

If we let the number of atoms with spin up and spin down be

$$N^{(+)} = \frac{1}{2}N + \delta, \quad N^{(-)} = \frac{1}{2}N - \delta, \quad (7.4)$$

the spin polarization parameter  $s$  is defined by

$$s = 2\delta/N = (N^{(+)} - N^{(-)}) / (N^{(+)} + N^{(-)}) = (N^{(+)} - N^{(-)}) / N. \quad (7.5)$$

The corresponding Fermi momenta for spin up and down are

$$k_F^{(+)} = k_F (1 + 2\delta/N)^{1/3} = k_F (1 + s)^{1/3}, \quad k_F^{(-)} = k_F (1 - 2\delta/N)^{1/3} = k_F (1 - s)^{1/3}, \quad (7.6)$$

where  $k_F$  is the Fermi momentum in the unpolarized system, given by Eq. (2.6). After expansion in powers of the polarization parameter  $\delta$ , the total kinetic energy of the system is, to second order in  $\delta$ ,

$$T_F(\delta) = N^{(+)} \frac{3}{10} (\hbar^2/M) k_F^{(+)}{}^2 + N^{(-)} \frac{3}{10} (\hbar^2/M) k_F^{(-)}{}^2 = \frac{3}{10} (\frac{1}{2} \hbar^2 k_F^2 / M) N (1 + \frac{20}{9} \delta^2 / N^2). \quad (7.7)$$

The total interaction energy in the polarized system can be written

$$V(\delta) = \sum_{k_i=0}^{k_F^{(+)}} \sum_{k_j=0}^{k_F^{(+)}} a_o(k_i, k_j) + \sum_{k_i=0}^{k_F^{(-)}} \sum_{k_j=0}^{k_F^{(-)}} a_o(k_i, k_j) + \sum_{k_i=0}^{k_F^{(+)}} \sum_{k_j=0}^{k_F^{(-)}} [a_e(k_i, k_j) + a_o(k_i, k_j)], \quad (7.8)$$

where the contributions from even and odd states are

$$a_e(k_i, k_j) = \sum_{\text{even } L} \langle k_{ij} | G_L(\rho) | k_{ij} \rangle, \quad a_o(k_i, k_j) = \sum_{\text{odd } L} \langle k_{ij} | G_L(\rho) | k_{ij} \rangle. \quad (7.9)$$

The statistical factor of 3 for odd  $L$  is here omitted from the  $G_L$ -matrix elements, while it has been included in our earlier definition of  $G_L$ . The factor of  $(2L+1)$  is still included as before, however.

Equation (7.8) can be rewritten in the form

$$V(\delta) = V(0) + \sum_{k_i=0}^{k_F} \left( \sum_{k_j=k_F}^{k_F^{(+)}} - \sum_{k_j=k_F}^{k_F^{(-)}} \right) [a_e(k_i, k_j) + 3a_o(k_i, k_j)] - \sum_{k_i=k_F}^{k_F^{(+)}} \sum_{k_j=k_F}^{k_F^{(+)}} [a_e(k_i, k_j) - a_o(k_i, k_j)], \quad (7.10)$$

where  $V(0)$  is the usual total interaction energy at equilibrium when  $\delta=0$ . The sum over  $k_i$  in the second term on the right-hand side is just like the single-particle potential

$$U(k_j) = \sum_{k_i=0}^{k_F} [a_e(k_i, k_j) + 3a_o(k_i, k_j)]. \quad (7.11)$$

Then for small  $\delta$  we have

$$\left( \sum_{k_j=k_F}^{k_F^{(+)}} - \sum_{k_j=k_F}^{k_F^{(-)}} \right) U(k_j) = 4\pi\Omega(2\pi)^{-3} (k_F^{(+)} - k_F^{(-)})^2 k_F^2 [\partial U(k)/\partial k]_{k=k_F}. \quad (7.12)$$

Equation (7.6) gives, to lowest order in  $\delta$ ,

$$k_F^{(+)} - k_F^{(-)} = \frac{1}{3} k_F (2\delta/N), \quad (7.13)$$

which, together with Eqs. (2.6) and (5.10), gives for Eq. (7.12) the expression

$$\left( \sum_{k_j=k_F}^{k_F^{(+)}} - \sum_{k_j=k_F}^{k_F^{(-)}} \right) U(k_j) = N \frac{2}{3} \hbar^2 k_F^2 (\delta/N)^2 (1/M^* - 1/M). \quad (7.14)$$

$$\text{Defining } a(k_F, k_F)_{\text{av}} = \left[ \int (d\Omega_i/4\pi) \int (d\Omega_j/4\pi) a(k_i, k_j) \right]_{k_i=k_j=k_F}, \quad (7.15)$$

we can write for the last term in Eq. (7.10)

$$\sum_{k_i=k_F}^{k_F^{(+)}} \sum_{k_j=k_F}^{k_F^{(+)}} [a_e(k_i, k_j) - a_o(k_i, k_j)] = N \frac{1}{3} (k_F^3/\pi^2) (\delta/N)^2 [a_e(k_F, k_F)_{\text{av}} - a_o(k_F, k_F)_{\text{av}}]. \quad (7.16)$$

Collecting the terms from Eqs. (7.7), (7.14), and (7.16), we then get the energy difference

$$E_o(\delta) = T_F(\delta) - T_F(0) + V(\delta) - V(0) = N \frac{2}{3} k_F^2 (\delta/N)^2 \left[ \hbar^2/M^* - \frac{1}{2} (k_F/\pi^2) [a_e(k_F, k_F)_{\text{av}} - a_o(k_F, k_F)_{\text{av}}] \right]. \quad (7.17)$$

As the Fermi liquid is polarized, the shift in the spin population will cause a change in the  $G$ -matrix elements through the change in the Fermi momentum. In the odd states, the Fermi momentum of the states with spin up shifts to  $k_F^{(+)}$  and with spin down to  $k_F^{(-)}$ . In even states, a particle with spin up interacts with a particle with spin down. When calculating the  $G$  matrix, Brueckner and Gammel here used an average value

$$k_F' = \left[ \frac{1}{2} (k_F^{(+)} + k_F^{(-)}) \right]^{\frac{1}{2}} \quad (7.18)$$

for the new Fermi momenta in the states of spin up and down. Indicating explicitly the dependence on the shifted Fermi momenta, we can rewrite Eq. (7.8) as

$$V(\delta) = \sum_{k_i=0}^{k_F^{(+)}} \sum_{k_j=0}^{k_F^{(+)}} a_0(k_i, k_j, k_F^{(+)}) + \sum_{k_i=0}^{k_F^{(-)}} \sum_{k_j=0}^{k_F^{(-)}} a_0(k_i, k_j, k_F^{(-)}) + \sum_{k_i=0}^{k_F^{(+)}} \sum_{k_j=0}^{k_F^{(-)}} [a_e(k_i, k_j, k_F') + a_0(k_i, k_j, k_F')]. \quad (7.19)$$

After carrying out an expansion of the amplitudes around  $k_F^{(+)}$ ,  $k_F^{(-)}$ , and  $k_F' = k_F$ , and keeping terms to second order in the small parameter  $\delta$ , we finally get an expression for the energy of the spin alignment  $E_\sigma$ , given as the ratio to the spin polarization energy  $E_{\sigma, F}$  of the ideal Fermi gas,

$$+ 2 \frac{M}{\hbar^2} \frac{k_F}{\pi^2} \left[ \int \frac{1}{4\pi k_F^3} d\vec{k}_i k_F \left( \frac{\partial a_0(k_i, k_j)}{\partial k_j} \right)_{k_j=k_F} + \frac{1}{8} \int \frac{1}{4\pi k_F^3} d\vec{k}_i \int \frac{1}{4\pi k_F^3} d\vec{k}_j k_F \right. \\ \left. \times \left( k_F \frac{\partial^2 a_e(k_i, k_j)}{\partial k_F^2} + 2 \frac{\partial a_e(k_i, k_j)}{\partial k_F} + 3k_F \frac{\partial^2 a_0(k_i, k_j)}{\partial k_F^2} - 6 \frac{\partial a_0(k_i, k_j)}{\partial k_F} \right) \right]. \quad (7.20)$$

The first term depending on the effective mass  $m^*$  comes from the change in the density of the single-particle levels. It arises from the momentum dependence of the single-particle potential and determines the quasiparticle specific-heat contribution. The second term comes directly from the spin dependence and arises from the change in the pair interaction as spins are shifted from antiparallel to parallel alignment. As the number of pairs with parallel spin increases, the exclusion principle requires that these pairs go into states of odd relative angular momentum. Then there is a net shift from even to odd states. The third term arises from the rearrangement terms in the single-particle energies, or the variation of the reaction matrix with the Fermi momentum because of the spin polarization.

To evaluate the last term in Eq. (7.20), i. e., the integrals inside the curly brackets, Brueckner and Gammel made the approximation

$$\partial a_e / \partial k_F \approx \partial a_0 / \partial k_F. \quad (7.21)$$

Since  $\partial a_e / \partial k_F$  appears with a much smaller coefficient than  $\partial a_0 / \partial k_F$ , one can hope that this assumption does not affect the results too much. They also assume that  $a_0$  depends only on  $|\vec{k}_i - \vec{k}_j|$ , i. e., on the relative momentum

$$k_0 = \frac{1}{2} |\vec{k}_i - \vec{k}_j|. \quad (7.22)$$

If we compare the results in Table VIII for even and odd  $L$ , we see that the assumption (7.21) is not at all valid. It is, in fact, so strongly violated that we have to consider  $\partial a_e / \partial k_F$  separately, even when it has a very small coefficient in front. After transforming the integrals in Eq. (7.20) to

$$\int d\vec{k}_i = 16\pi \int_0^{k_F} k_0^2 (1 - k_0/k_F) dk_0, \quad \int d\vec{k}_i \int d\vec{k}_j = 32\pi \left( \frac{4}{3} \pi k_F^3 \right) \int_0^{k_F} k_0^2 (1 - \frac{3}{2} k_0/k_F + \frac{1}{2} k_0^3/k_F^3) dk_0, \quad (7.23)$$

the third term in Eq. (7.20) can be written as

$$I = \frac{k_F M}{\pi^2 \hbar^2} \int_0^{k_F} dk_0 \frac{k_0^2}{k_F^2} \left[ \left( \frac{2}{3} - \frac{k_0}{k_F} + \frac{1}{3} \frac{k_0^3}{k_F^3} \right) \left( k_F \frac{\partial^2 a_e(k_0, k_F)}{\partial k_F^2} + 3k_F \frac{\partial^2 a_0(k_0, k_F)}{\partial k_F^2} - 2 \frac{\partial a_e(k_0, k_F)}{\partial k_F} \right) \right. \\ \left. + \left( 4 - 2 \frac{k_0}{k_F} - 2 \frac{k_0^3}{k_F^3} \right) \frac{\partial a_0(k_0, k_F)}{\partial k_F} \right]. \quad (7.24)$$

If we assume a linear dependence of  $a$  on  $k_F$ , we can write

$$a_e(x, k_F) = a_e(x, 0) + k_F f_e(x), \quad a_0(x, k_F) = a_0(x, 0) + k_F f_0(x), \quad (7.25)$$

where  $x = k_0/k_F$ ,

$$(7.26)$$

TABLE VIII. Diagonal  $G_L$ -matrix elements in  $\text{\AA}$ , calculated on the energy shell. BG method is with the exclusion principle included; RS method is with the exclusion principle neglected. Yntema-Schneider potential.  $k_0$  is varied.  $\Delta=0.4$ .  $m_0^*=2.5$ .

$k_F(\text{\AA}^{-1})$	$k_0/k_F$	BG method		RS method		Difference, BG - RS	
		$\sum_{\text{even } L} G_L$	$\sum_{\text{odd } L} G_L$	$\sum_{\text{even } L} G_L$	$\sum_{\text{odd } L} G_L$	$\sum_{\text{even } L} G_L$	$\sum_{\text{odd } L} G_L$
0.75	0.125	9.42	-4.10	-8.25	-4.24	17.67	0.14
	0.25	19.26	-13.22	1.33	-13.72	17.93	0.50
	0.375	28.69	-21.71	10.20	-22.58	18.49	0.87
	0.50	34.40	-26.33	14.95	-27.41	19.45	1.08
	0.625	35.59	-26.08	14.78	-27.10	20.81	1.02
	0.75	32.40	-21.27	9.99	-22.00	22.41	0.73
	0.875	25.99	-13.37	2.02	-13.77	23.97	0.40
	1.00	18.30	-4.35	-6.96	-4.68	25.26	0.33
	0.78	0.125	16.36	-4.39	-6.15	-4.53	22.51
0.25		26.55	-13.92	3.84	-14.41	22.71	0.49
0.375		35.83	-22.36	12.64	-23.20	23.19	0.84
0.50		40.87	-26.39	16.82	-27.41	24.05	1.02
0.625		40.88	-25.10	15.67	-26.05	25.21	0.95
0.75		36.33	-19.09	9.82	-19.77	26.51	0.68
0.875		28.75	-10.20	1.15	-10.58	27.60	0.38
1.00		20.24	-0.65	-7.96	-0.99	28.20	0.34

which gives

$$\frac{\partial a_e(x, k_F)}{\partial k_F} = f_e(x) = \frac{a_e(x, k_F) - a_e(x, 0)}{k_F}, \quad \frac{\partial a_o(x, k_F)}{\partial k_F} = f_o(x) = \frac{a_o(x, k_F) - a_o(x, 0)}{k_F}. \quad (7.27)$$

In Eq. (7.25),  $a_{e,o}(x, 0)$  is the amplitude for zero density, for which we take the RS results with the exclusion principle neglected. The quantity  $a_{e,o}(x, k_F)$  is the amplitude at the equilibrium density, for which we take the corresponding BG results. Tables VI, VII, and VIII give a comparison between these two cases, as we have seen. It turns out, however, that the assumption (7.27) is a bad approximation. Both the first and second derivatives in Eq. (7.24) have to be estimated numerically, and details will be published later.

To obtain the second term in Eq. (7.20), we use the results given in Table IX. These results differ from earlier values for  $G_L$ -matrix elements by a factor of 3 for odd  $L$  states, because of our definition (7.9). Using Eq. (7.22) for  $k_i = k_j = k_F$ , we write

$$k_0 = k_F \sin(\frac{1}{2}\theta), \quad (7.28)$$

and average the  $G$ -matrix elements over the Fermi surface.

With  $M^*/M=2.5$ , the final results for Eq. (7.20) are

$$\begin{aligned} E_\sigma/E_{\sigma, F} &= 0.40 - 1.25 + 0.95 = 0.10 \quad \text{for } k_F = 0.75 \text{ \AA}^{-1}, \\ &= 0.40 - 1.40 + 1.05 = 0.05 \quad \text{for } k_F = 0.78 \text{ \AA}^{-1}, \end{aligned} \quad (7-29)$$

which gives us a magnetic susceptibility ratio of

$$\chi/\chi_F \approx 10 \quad (7.30)$$

for  $k_F = 0.75 \text{ \AA}^{-1}$ . This result is very approximate, but should indicate the correct order of magnitude at least. However, we notice that the set of results for  $k_F = 0.78 \text{ \AA}^{-1}$  gives a susceptibility ratio of 20, and that it is a rather uncertain value.

Brueckner and Gammel got a result of

$$E_\sigma/E_{\sigma, F} = 0.543 - 0.780 + 0.320 = 0.083, \quad (7.31)$$

TABLE IX. Diagonal  $G_L$ -matrix elements in  $\text{\AA}$ , calculated on the energy shell. Yntema-Schneider potential.  $k_0$  is varied.  $m_0^*=2.5$ .

$k_F(\text{\AA}^{-1})$	$k_0/k_F$	$\Delta=0.3$			$\Delta=0.4$		
		$\sum_{\text{even } L} G_L$	$\sum_{\text{odd } L} G_L$	Difference	$\sum_{\text{even } L} G_L$	$\sum_{\text{odd } L} G_L$	Difference
0.75	0.001	-2.1	0	-2.1	5.1	0	5.1
	0.125	2.3	-4.1	6.4	9.4	-4.1	13.5
	0.25	12.3	-13.4	25.7	19.3	-13.2	32.5
	0.375	22.0	-22.1	44.1	28.7	-21.7	50.4
	0.50	28.1	-27.0	55.1	34.4	-26.3	60.7
	0.625	29.7	-27.1	56.8	35.6	-26.1	61.7
	0.75	26.9	-22.6	49.5	32.4	-21.3	53.7
	0.875	20.9	-15.1	36.0	26.0	-13.4	39.4
	1.00	13.6	-6.5	20.1	18.3	-4.4	22.7
	0.78	0.001	3.8	0	3.8	11.7	0
0.125		8.5	-4.4	12.9	16.4	-4.4	20.8
0.25		18.9	-14.1	33.0	26.6	-13.9	40.5
0.375		28.5	-22.8	51.3	35.8	-22.4	58.2
0.50		34.0	-27.2	61.2	40.9	-26.4	67.3
0.625		34.4	-26.3	60.7	40.9	-25.1	66.0
0.75		30.4	-20.7	51.1	36.3	-19.1	55.4
0.875		23.3	-15.9	39.2	28.8	-10.2	39.0
1.00		15.3	-3.1	18.4	20.2	-0.7	20.9

or  $\chi/\chi_F=12$  for  $k_F=0.74 \text{\AA}^{-1}$ . Our first term in Eq. (7.29) is of the same order as the first term in Eq. (7.31), but the second and third terms are completely different. It seems quite impossible to reproduce the second and third term in the expression (7.31) of Brueckner and Gammel, even from their own data and in the way they claim the calculations are done. Their second term is too small for some reason, and their third term is too small because of the approximation (7.21).

The susceptibility is also often given as

$$\chi = C_C / T^* = \frac{3}{2} C_C / T_F^{**}, \quad (7.32)$$

where  $C_C$  is the Curie constant,  $T^*$  is the effective magnetic temperature, and  $T_F^{**}$  is the Fermi temperature or the magnetic degeneracy temperature. Experimental values for the spin susceptibility ratio are the  $T_F^{**}=0.55^\circ\text{K}$  or  $\chi/\chi_F=9.0$  of Beal and Hatton,<sup>27</sup> the  $T^*=0.35^\circ\text{K}$  or  $\chi/\chi_F=9.5$  of Anderson *et al.*,<sup>7,28,29</sup> and the  $T_F^{**}=0.43^\circ\text{K}$  or  $\chi/\chi_F=11.5$  of Thomson *et al.*<sup>30</sup> Another theoretical value is the  $\chi/\chi_F=13.9$  of Woo.<sup>15</sup>

The magnetic susceptibility is thus found to be rather close to experimental values. The energy required to polarize the spins is very small compared to that for a Fermi gas, and the corresponding magnetic susceptibility is very large. The large magnetic susceptibility is due to the large spin-dependent terms in Eq. (7.20). It arises from a ferromagnetic exchange interaction tending to line up the nuclear spins parallel, and hence tending to cancel the antiparallel alignment due to Fermi-Dirac statistics. This large spin-spin interaction comes from the exclusion principle, and is not purely a magnetic spin-spin effect. Since the effective mass increases with increasing density, the magnetic susceptibility should also increase in the same way. This is, in fact, indicated by our results.

## 8. NEW POTENTIAL

The interatomic potential used seems to have a strong influence on the results of the calculations. Potentials with different shapes generally give different results, and the value we obtain for the binding energy is extremely sensitive to changes in the various parts of the potential. This is because the binding energy is really a small difference between large repulsive and attractive terms. The repulsive core in the potential is not at all well known, and this uncertainty may cause relatively large

errors in the calculations. So we want to discuss this question in more detail.

Helium atoms have rigid electron shells, as indicated by a dielectric constant nearly equal to unity. Because of this, the force acting between two distant atoms in liquid  $^3\text{He}$  is almost exactly equal to the force between two isolated helium atoms. The polarizability of each of the interacting atoms is practically unchanged by the presence of neighboring atoms, and the polarization of the intervening atoms does not change the interaction force between the atoms which we consider. How-

ever, although the energy of interaction between the atoms in the liquid at large distances is close to the interaction energy for isolated atoms, the scattering amplitude for the excitations is not at all similar to that for atoms, since interaction with neighboring atoms has a considerable influence on the excitation motion. The van der Waals forces are connected with the existence of zero-point fluctuations of long-wave electromagnetic radiation in the medium, i. e., with the exchange of virtual long-wave photons.

A good potential function should satisfy the following criteria. It should go asymptotically to zero as  $r \rightarrow \infty$ , it should become infinite at  $r = 0$ , and it should have a minimum between. The limit infinity for  $r \rightarrow 0$  is, however, not strictly true if nuclear structure and forces are taken into account. Then one can consider the potential energy as the algebraic sum of different parts; one the nuclear repulsive potential corresponding to a Coulomb potential, the other the purely electronic energy. Van der Waals forces introduce terms of the form  $r^{-n}$ .

Varshni<sup>31</sup> has made a comparative study of many potential functions for diatomic molecules. Among others he refers to the Frost-Musulin potential, constructed from semitheoretical arguments, of the form

$$V(r) = [(b/r) - c] \exp(-ar), \quad (8.1)$$

for which Frost and Musulin<sup>32</sup> got quite satisfactory results for hydrogen. We shall return to this potential form later.

The interaction energy between two normal helium atoms as a function of the internuclear distance  $r$  has been calculated quantum mechanically by several authors. Davison<sup>33</sup> has calculated the coefficients of the series representation of the long-range interaction potential between two atomic systems by a variational procedure, using highly refined ground-state wave functions. Earlier values for dipole-dipole polarization or  $r^{-6}$  terms were obtained by use of sets of oscillator strength data adjusted to reproduce the experimental refractive indices and to satisfy the Thomas-Reiche-Kuhn sum rule. Davison checked his method by calculation of dipole and quadrupole polarizabilities, and then calculated the dispersion terms in the two-body potential. The values are 1.47 atomic units for the dipole-dipole or  $r^{-6}$  term, and 14.2 atomic units for the dipole-quadrupole or  $r^{-8}$  term. Other values given for the first coefficient are 1.46 by Kingston,<sup>34</sup> 1.47 by Bell,<sup>35</sup> and 1.49 by Barker and Leonard.<sup>36</sup> The variational procedure is successful in refined calculations of multipole polarizabilities, and the values obtained can be expected to be of fairly high accuracy, but are generally not in agreement with values previously derived from the viscosity, second virial coefficients, and low-energy scattering of atomic beams.

The second virial coefficient is found to be a sensitive test of the semiempirical potentials constructed. There are, however, limitations because of quantum corrections. Another test of derived potentials could be to require a simultaneous fit of the second virial coefficient and the

transport coefficients.

The repulsive potential between two ground-state helium atoms has been investigated by several people. Theoretical self-consistent field calculations of the helium-helium interaction at small distances have been performed by Phillipson,<sup>37</sup> and Gilbert and Wahl.<sup>38</sup> Potential energy curves in the repulsive region are calculated, using single-configuration wave functions constructed from molecular orbitals, and then further refined to include effects of electron correlations by inclusion of superposition of configurations. In the molecular orbit approach, the two helium atoms are regarded as a helium molecule in which each of the electrons is assigned to a one-electron orbital wave function, or molecular orbit which extends over the whole molecule.

The repulsive part of the potential energy curve has been studied experimentally by the atomic-beam scattering method of Jordan and Amdur.<sup>39</sup> They have measured the total elastic cross sections for helium atoms which have been scattered by helium at room-temperature. It is a scattering experiment involving high-velocity neutral beams of helium atoms in ground states, and it gives results for the potential in the range  $0.6 < r < 1.1 \text{ \AA}$ . The results seem to indicate a remaining uncertainty in theoretical calculations at short ranges.

There has always been bad agreement between short-range potentials for helium obtained from scattering and those from theoretical calculations. One could argue that the atomic-beam potentials are in principle not strictly adiabatic, since at higher energies the nuclear motion of the system is not negligibly small compared to the orbital motion of the electrons. The potentials derived from scattering experiments may be velocity-dependent, and not characteristic of two helium atoms fixed in space with specified internuclear separations. However, there seems to be no significant difference between the potential obtained from scattering and a calculated adiabatic potential. When examining helium potentials, we find that semiempirical curves lie about 10% below theoretical ones in the repulsive region. The theoretical errors can be classified in three main categories as correlation errors, expansion errors, and distortion errors. But there is at the moment no reliable method for estimating the magnitude of these errors. It just seems that theoretical curves give too much repulsion.

But theoretical calculations of the short-range repulsion and of the coefficients of the multipoles in the long-range attraction between helium atoms have been considerably improved recently. Bernstein and Morse<sup>40</sup> suggested an interpolation method to infer the helium-helium interaction at all distances. They constructed a potential by joining Phillipson's short-range repulsion<sup>37</sup> via a Morse function to a long-range attraction given by Dalgarno and Kingston.<sup>41</sup> But Varshni<sup>42</sup> has calculated the second virial coefficient for their potential, and finds rather poor agreement with experimental data below 150°K.

Bruch and McGee<sup>10</sup> have made a detailed study of the construction of a semiempirical helium-helium interaction by the same procedure. They

use an empirical potential function to interpolate through the potential minimum between theoretical calculations at short and long separations. The parameters in this function are restricted by the requirement of slope matching at the end points of the interpolation. The final potential is then given by three separate analytic terms for the three ranges of separations. However, Bruch and McGee found that they had to modify this procedure because potentials constructed in this way do not describe thermodynamic data satisfactorily; for instance, second virial coefficients calculated for these potentials are in poor agreement with experimental data. They therefore modified the original interpolation method by constructing a semiempirical potential which fits the data well. A three-parameter potential is joined by slope matching to the theoretical long-range interaction only.

The long-range interaction is assumed to be given by the first two nonzero terms in a multipole expansion, i. e., the dipole-dipole and dipole-quadrupole interactions. This potential energy is given as a function of the nuclear separation  $r$  as

$$V_L(r) = -C_6 r^{-6} - C_8 r^{-8}. \quad (8.2)$$

The values of the constants  $C_6$  and  $C_8$  are

$$\begin{aligned} C_6 &= 1.47 \text{ a. u.} = 1.41 \times 10^{-60} \text{ erg cm}^6, \\ C_8 &= 14.2 \text{ a. u.} = 3.82 \times 10^{-76} \text{ erg cm}^8, \end{aligned} \quad (8.3)$$

as given by Davison.<sup>33</sup> Higher multipoles and an overlap repulsion are then neglected, but they should partially cancel each other.

Bruch and McGee then relax the original requirements in order to fit the experimental second virial coefficients. The potential is only required to make a first-order contact with the theoretical long-range interaction, which means

$$\begin{aligned} V(r) &= V_S(r) \text{ for } r \leq r_2, \\ &= V_L(r) \text{ for } r > r_2. \end{aligned} \quad (8.4)$$

The parameters of the best semiempirical potential finally derived by Bruch and McGee are practically the same as the parameters listed for their so-called Frost-Musulin potential. This should then be the analytic form for a semiempirical potential which seems to fit the virial data most closely, and it is given as

$$V_S = -\epsilon [1 + c(1 - x^{-1})] \exp[-c(x - 1)], \quad (8.5)$$

where  $x = r/R$ ,  $R = 2.98 \text{ \AA}$ ,  $c = 8.01$ ,

$$\epsilon = 1.73 \times 10^{-15} \text{ erg} = 12.5^\circ \text{K}. \quad (8.6)$$

We will use this potential in some new calculations of the binding energy.

## 9. CALCULATIONS WITH NEW POTENTIAL

We have repeated our calculations of the two-body and the three-body contribution to the binding energy of liquid  $^3\text{He}$  using the new potential (8.2) and (8.5). Our new potential is defined as

$$\begin{aligned} V_{FM}(r) &= -12.54 \left[ 1 + 8.01 \left( 1 - \frac{2.98}{r} \right) \right] \\ &\times e^{8.01(1 - r/2.98)}, \quad \text{for } r < 3.5 \text{ \AA}, \\ &= -7250 \left[ \frac{1.41}{r^6} + \frac{3.82}{r^8} \right], \quad \text{for } r > 3.5 \text{ \AA}, \end{aligned} \quad (9.1)$$

in  $^\circ\text{K}$ , where  $r$  is measured in  $\text{\AA}$ . We will call this our Frost-Musulin potential. Figure 10 shows this potential together with the Yntema-Schneider potential defined by Eq. (2.8).

Calculations are performed as outlined and explained in I, II, and Sec. 2 of this paper; and results are given in Tables X-XIV.

We get a binding energy of  $-2.0^\circ\text{K}$  per particle for  $r_0 = 2.46 \text{ \AA}$  or  $k_F = 0.78 \text{ \AA}^{-1}$ . The corresponding experimental values are  $-2.5^\circ\text{K}$  per particle for  $r_0 = 2.43 \text{ \AA}$  or  $k_F = 0.79 \text{ \AA}^{-1}$ . Our theoretical result thus is fairly close to the experimental result, but this agreement should not be taken too seriously, of course. There are too many uncertainties involved in the calculations. It is, however, an encouraging result, and indicates that there is still hope for a good reproduction of experimental values by theoretical calculations, using methods originated by Brueckner, Bethe, and collaborators.

## 10. SUMMARY

Our results have been discussed and compared with other results separately in the various sec-

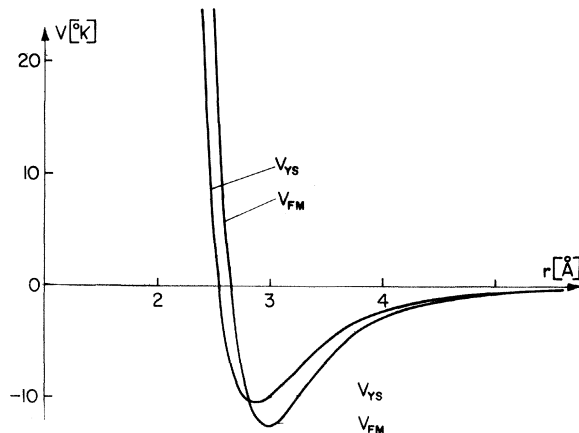


FIG. 10. Potentials for liquid He.  $V_{YS}$  (Yntema-Schneider) is given by Eq. (2.8) and  $V_{FM}$  (Frost-Musulin) by Eq. (9.1).



TABLE X. Diagonal  $G_L$ -matrix elements in  $\text{\AA}$ , calculated on the energy shell. Statistical weights included. Frost-Musulin potential.  $k_0$  is varied.  $\Delta=0.5$   $m_0^*=2.5$ .

$k_F$ ( $\text{\AA}^{-1}$ )	$k_0/k_F$	$L=0$	$L=1$	$L=2$	$L=3$	$L>3$	Total
0.75	0.001	5.3	0	0	0	0	5.3
	0.125	10.6	-14.6	-0.1	0	0	-4.1
	0.25	23.9	-47.1	-1.6	-0.3	0	-25.0
	0.375	39.7	-75.7	-5.5	-2.2	-0.5	-44.3
	0.50	53.3	-86.8	-11.5	-7.3	-1.9	-54.2
	0.625	62.4	-76.8	-18.0	-15.3	-4.3	-51.9
	0.75	66.2	-47.2	-24.0	-25.6	-7.8	-38.5
	0.875	64.6	-3.3	-27.9	-38.4	-12.8	-17.7
1.00	58.8	46.8	-28.4	-52.6	-19.5	5.2	
0.78	0.001	14.1	0	0	0	0	14.1
	0.125	19.8	-15.7	-0.1	0	0	4.0
	0.25	33.7	-49.5	-1.8	-0.4	-0.1	-17.9
	0.375	49.7	-77.4	-6.2	-2.7	-0.6	-37.2
	0.50	62.8	-85.6	-12.4	-8.4	-2.2	-45.8
	0.625	70.8	-70.8	-19.2	-17.1	-4.8	-41.1
	0.75	72.9	-35.6	-25.0	-28.4	-8.9	-25.0
	0.875	69.3	13.2	-28.2	-42.1	-14.4	-2.1
1.00	61.5	66.2	-27.3	-56.8	-21.9	21.8	

tions, but we would like to add some comments.

The binding energy of liquid  $^3\text{He}$  is calculated to be  $-1.0^\circ\text{K}$  per particle for the Yntema-Schneider<sup>11</sup> potential given by Brueckner and Gammel,<sup>1</sup> and  $-2.0^\circ\text{K}$  per particle for the Frost-Musulin<sup>32</sup> potential given by Bruch and Mc Gee.<sup>10</sup> The results of our calculations can be compared with values from other calculations, as we have done in Sec. 2, and we want to mention the other methods being applied.

Using the temperature-dependent many-body Green's function formalism of Martin and Sch-

winger,<sup>43</sup> Beck and Sessler<sup>14</sup> have calculated low-temperature properties of liquid  $^3\text{He}$ . Their Green's function formalism gives an infinite set of coupled integral equations, which must be solved self-consistently. It is impossible in practice to solve this set of equations exactly, and approximations must be made. Using separable potentials and a noninteracting spectral function to define the two-body interaction in the medium in a preliminary zero-temperature calculation, they obtain a spectral function and self-energy for quasiparticles. Thermodynamical properties of the

TABLE XI. Diagonal  $G_L$ -matrix elements in  $\text{\AA}$ , calculated on the energy shell. Statistical weights included. Frost-Musulin potential.  $k_0$  is varied.  $\Delta=0.6$ .  $m_0^*=2.5$ .

$k_F$ ( $\text{\AA}^{-1}$ )	$k_0/k_F$	$L=0$	$L=1$	$L=2$	$L=3$	$L>3$	Total
0.75	0.001	13.5	0	0	0	0	13.5
	0.125	18.8	-14.5	-0.1	0	0	4.2
	0.25	31.8	-46.4	-1.6	-0.3	0	-16.5
	0.375	47.2	-74.2	-5.5	-2.2	-0.5	-35.3
	0.50	60.4	-84.4	-11.4	-7.3	-1.9	-44.6
	0.625	69.0	-73.3	-17.9	-15.2	-4.3	-41.7
	0.75	72.1	-42.4	-23.8	-25.6	-7.8	-27.5
	0.875	69.9	2.6	-27.6	-38.2	-12.8	-6.0
1.00	63.5	53.8	-27.9	-52.3	-19.5	17.7	
0.78	0.001	23.2	0	0	0	0	23.2
	0.125	28.8	-15.5	-0.1	0	0	13.2
	0.25	42.5	-48.7	-1.8	-0.4	-0.1	-8.5
	0.375	58.0	-75.8	-6.1	-2.7	-0.6	-27.2
	0.50	70.6	-82.8	-12.4	-8.4	-2.2	-35.2
	0.625	77.9	-66.7	-19.1	-17.1	-4.8	-29.8
	0.75	79.2	-30.2	-24.7	-28.3	-8.9	-12.8
	0.875	75.0	19.9	-27.8	-41.9	-14.4	10.8
1.00	66.4	74.1	-26.8	-56.4	-21.9	35.5	

TABLE XII. Binding energy for liquid  $\text{He}^3$  in  $^\circ\text{K}$ . Only two-body terms included. Frost-Musulin potential.  $\Delta$  and  $m_0^*$  are varied.

$k_F$ ( $\text{\AA}^{-1}$ )	$\Delta$	0.4		0.5	
		$m_0^*$	2.0	2.5	2.0
0.75		-0.51	-0.42	0.08	0.17
0.78		-0.12	-0.01	0.61	0.72

system are then calculated, using this spectral function. Beck<sup>13</sup> continued the program by calculating zero-temperature properties, using the local potential of Bernstein and Morse.<sup>40</sup> A zero-order solution of the thermodynamically consistent approximation is obtained from noninteracting spectral functions. Afterwards an iterative solution of the coupled integral equations is obtained, giving a spectral function for the interacting system. But the calculated properties are in bad agreement with experimental values, possibly because of the potential being used.

Wu and Feenberg<sup>44</sup> have a rather different approach to the problem. They relate liquid  $^3\text{He}$  to a boson system of particles of the same mass; and given the properties of the boson system, they get a rapidly convergent approximation for the fermion system. Suggesting a two-body correlative approximation to the boson system, which can be checked against experiments on liquid  $^4\text{He}$ , they repeat the calculations for bosons of mass 3. In this way a theory of the normal ground state of liquid  $^3\text{He}$  is constructed, using matrix elements in a representation of correlated basis functions. Wu and Feenberg calculate the fermion radial distribution function, and get a connection between known results for the fermion and boson forms of the hard-sphere system at low density and also get properties of a hypothetical fermion  $^4\text{He}$  system. In a second paper, Feenberg and Woo<sup>45</sup> evaluate matrix elements of the interacting system by a cluster-expansion technique. They construct an orthonormal basis to express the Hamiltonian operator in quasiparticle form. The methods are then used by Woo<sup>15</sup> in a calculation of the ground-state properties of liquid  $^3\text{He}$ . More recently Schiff and Verlet<sup>16</sup> have made a variational calculation of the ground-state energy of liquid  $^3\text{He}$ , using Jastrow-type trial wave functions.

TABLE XIII. Three-body energy terms for liquid  $\text{He}^3$  in  $^\circ\text{K}$ . Frost-Musulin potential.  $k_0 = 0.55 k_F$  on the energy shell.  $k_0$  is varied off the energy shell.  $\Delta = 0.5$ .  $m_0^* = 2.5$ .

$k_F$ ( $\text{\AA}^{-1}$ )	$k_0/k_F$	0.6	0.8	1.0	1.2
		0.75	-2.09	-2.41	-2.06
0.78		-2.40	-2.95	-2.31	-0.63

The energy expectation value is calculated approximately by use of the cluster expansion developed by Wu and Feenberg, up to second order. This expansion seems to converge rapidly, and should not depend too much on variational parameters. Assuming a Lennard-Jones 6-12 potential with de Boer-Michels parameters,<sup>46</sup> Massey and Woo<sup>17</sup> have also recently calculated the ground-state energy by the variational procedure connected with the method of correlated basis functions. They obtain a rather small binding energy, but show that a second-order perturbation correction added to the result of Schiff and Verlet will give a binding energy of  $-1.6^\circ\text{K}$  per particle.

We have earlier made some comments about Brueckner's papers on liquid  $^3\text{He}$ , since one of our main justifications for the present work is to check, modify, and possibly improve the Brueckner method. Although the Brueckner theory does not include the possible existence of a superfluid phase, it should describe the liquid quite well at temperatures above the transition temperature, since most of the properties of liquid  $^3\text{He}$  change slowly with temperature. Moreover, possible singularities occur only for states with energies very close to the Fermi surface, and these make a negligible contribution to the bulk properties of the liquid (except for the specific heat). If these states are ignored or treated in an approximate way, the error should be small.

#### ACKNOWLEDGMENTS

The author would like to thank Professor G. E. Brown for helpful suggestions and stimulating discussions. He also would like to thank Dr. H. S. Picker for kindly reading and criticizing the manuscript.

TABLE XIV. Binding energy for liquid  $^3\text{He}$  in  $^\circ\text{K}$ . Frost-Musulin potential.  $W_N$  is the interaction energy from the  $N$ -body term.  $E_B$  is the binding energy with only two-body terms included, and  $B_E$  is the total binding energy.  $m_0^* = 2.5$ .

$k_F$ ( $\text{\AA}^{-1}$ )	$r_0$ ( $\text{\AA}$ )	$\rho$ ( $\text{\AA}^{-3}$ )	$\Delta$	$W_2$ ( $^\circ\text{K}$ )	$T$ ( $^\circ\text{K}$ )	$E_B$ ( $^\circ\text{K}$ )	$W_3$ ( $^\circ\text{K}$ )	$B_E$ ( $^\circ\text{K}$ )
0.75	2.56	0.0142	0.45	-3.00	2.75	-0.25	-1.70	-1.95
0.78	2.46	0.0160	0.41	-3.05	3.00	-0.05	-1.95	-2.00

\*Work supported in part by the U. S. Atomic Energy Commission and the Higgins Scientific Trust Fund.

†Present address: Institute for Pure and Applied Physical Sciences, University of California, San Diego, La Jolla, California.

<sup>1</sup>K. A. Brueckner and J. L. Gammel, Phys. Rev. 109, 1040 (1958); 121, 1863 (1961).

<sup>2</sup>R. H. Sherman and F. J. Edeskuty, Ann. Phys. (N. Y.) 9, 522 (1960).

<sup>3</sup>T. R. Roberts, R. H. Sherman, and S. G. Sydorik, J. Res. Natl. Bur. Std. 68A, 567 (1964).

<sup>4</sup>W. R. Abel, A. C. Anderson, W. C. Black, and J. C. Wheatley, Phys. Rev. Letters 15, 875 (1965).

<sup>5</sup>K. A. Brueckner and K. R. Atkins, Phys. Rev. Letters 1, 315 (1958).

<sup>6</sup>C. Boghosian, H. Meyer, and J. E. Rives, Phys. Rev. 146, 110 (1966).

<sup>7</sup>A. C. Anderson, D. O. Edwards, W. R. Roach, E. Sarwinski, and J. C. Wheatley, Phys. Rev. Letters 17, 367 (1966).

<sup>8</sup>E. Østgaard, Phys. Rev. 170, 257 (1968).

<sup>9</sup>E. Østgaard, Phys. Rev. 171, 248 (1968).

<sup>10</sup>L. M. Bruch and I. J. McGee, J. Chem. Phys. 46, 2959 (1967).

<sup>11</sup>J. L. Yntema and W. G. Schneider, J. Chem. Phys. 18, 641, 646 (1950).

<sup>12</sup>E. C. Kerr and R. D. Taylor, Ann. Phys. (N. Y.) 20, 450 (1962).

<sup>13</sup>D. E. Beck, Phys. Rev. 160, 250 (1967).

<sup>14</sup>D. E. Beck and A. M. Sessler, Phys. Rev. 146, 161 (1966).

<sup>15</sup>(a) C.-W. Woo, Phys. Rev. 151, 138 (1966); (b) private communication.

<sup>16</sup>D. Schiff and L. Verlet, Phys. Rev. 160, 208 (1967).

<sup>17</sup>W. E. Massey and C.-W. Woo, Phys. Rev. 164, 256 (1967).

<sup>18</sup>M. Kirson, Nucl. Phys. A99, 353 (1967).

<sup>19</sup>H. A. Bethe, B. H. Brandow, and A. G. Petschek, Phys. Rev. 129, 225 (1963).

<sup>20</sup>H. A. Bethe and J. Goldstone, Proc. Roy. Soc. (London) A238, 551 (1957).

<sup>21</sup>N. M. Hugenholtz and L. Van Hove, Physica 24, 363 (1958).

<sup>22</sup>K. S. Masterson and K. Sawada, Phys. Rev. 133,

A1234 (1964).

<sup>23</sup>A. C. Anderson, G. L. Salinger, W. A. Steyert, and J. C. Wheatley, Phys. Rev. Letters 7, 295 (1961).

<sup>24</sup>L. Goldstein, Phys. Rev. 117, 375 (1960).

<sup>25</sup>D. F. Brewer and J. G. Daunt, Phys. Rev. 115, 843 (1959).

<sup>26</sup>J. E. Rives and H. Meyer, Phys. Rev. Letters 7, 217 (1961).

<sup>27</sup>B. T. Beal and J. Hatton, Phys. Rev. 139, A1751 (1965).

<sup>28</sup>A. C. Anderson, W. Reese, R. J. Sarwinski, and J. C. Wheatley, Phys. Rev. Letters 7, 220 (1961).

<sup>29</sup>A. C. Anderson, W. Reese and J. C. Wheatley, Phys. Rev. 127, 671 (1962).

<sup>30</sup>A. L. Thomson, H. Meyer, and E. D. Adams, Phys. Rev. 128, 509 (1962).

<sup>31</sup>Y. P. Varshni, Rev. Mod. Phys. 29, 661 (1957); 31, 839 (1959).

<sup>32</sup>A. A. Frost and B. Musulin, J. Chem. Phys. 22, 1017 (1954).

<sup>33</sup>W. D. Davison, Proc. Phys. Soc. (London) 87, 133 (1966).

<sup>34</sup>A. E. Kingston, Phys. Rev. 135, A1018 (1964).

<sup>35</sup>R. J. Bell, Proc. Phys. Soc. (London) 86, 17 (1965).

<sup>36</sup>J. A. Barker and P. J. Leonard, Phys. Letters 13, 27 (1964).

<sup>37</sup>P. E. Phillipson, Phys. Rev. 125, 1981 (1962).

<sup>38</sup>T. L. Gilbert and A. C. Wahl, J. Chem. Phys. 47, 3425 (1967).

<sup>39</sup>J. E. Jordan and I. Amdur, J. Chem. Phys. 46, 165 (1967).

<sup>40</sup>R. B. Bernstein and F. A. Morse, J. Chem. Phys. 40, 917 (1964).

<sup>41</sup>A. Dalgarno and A. E. Kingston, Proc. Phys. Soc. (London) 78, 607 (1961).

<sup>42</sup>Y. P. Varshni, J. Chem. Phys. 45, 3894 (1966).

<sup>43</sup>P. C. Martin and J. Schwinger, Phys. Rev. 115, 1342 (1959).

<sup>44</sup>F. Y. Wu and E. Feenberg, Phys. Rev. 128, 943 (1962).

<sup>45</sup>E. Feenberg and C.-W. Woo, Phys. Rev. 137, A391 (1965).

<sup>46</sup>J. de Boer and A. Michels, Physica 5, 945 (1938).